Modified Heider balance on Erdös-Rényi networks

R. Masoumi,[1] F. Oloomi,[1] S. Sajjadi,[2,3] A. H. Shirazi,[1] and G. R. Jafari[1,4,*]

[1]*Department of Physics, Shahid Beheshti University, Evin, Tehran 19839, Iran*

[2]*Complexity Science Hub Vienna, Vienna, Austria*

[3]*Central European University, Vienna, Austria*

[4]*Institute of Information Technology and Data Science, Irkutsk National Research Technical University, 83, Lermontova Street, 664074 Irkutsk, Russia*

(Received 28 March 2022; revised 16 August 2022; accepted 22 August 2022; published 8 September 2022)

The lack of signed random networks in standard balance studies has prompted us to extend the Hamiltonian of the standard balance model. Random networks with tunable parameters are suitable for better understanding the behavior of standard balance as an underlying dynamics. Moreover, the standard balance model in its original form does not allow preserving tensed triads in the network. Therefore, the thermal behavior of the balance model has been investigated on a fully connected signed network recently. It has been shown that the model undergoes an abrupt phase transition with temperature. Considering these two issues, we examine the thermal behavior of the structural balance model defined on Erdös-Rényi random networks within the range of their connected regime. We provide a mean-field solution for the model. We observe a first-order phase transition with temperature for a wide range of connection probabilities. We detect two transition temperatures, $T_{\rm cold}$ and $T_{\rm hot}$, characterizing a hysteresis loop. We find that with decreasing the connection probability, both $T_{\rm cold}$ and $T_{\rm hot}$ decrease. However, the slope of decreasing $T_{\rm hot}$ with decreasing connection probability is larger than the slope of decreasing $T_{\rm cold}$. Hence, the hysteresis region gets narrower until it disappears in a certain connection probability. We provide a phase diagram in the temperature-tie density plane to accurately observe the metastable or coexistence region behavior. Then we justify our mean-field results with a series of Monte Carlo simulations.

DOI: 10.1103/PhysRevE.106.034309

I. INTRODUCTION

Network models are a powerful method for describing complex phenomena. Networks represent systems as a set of nodes and ties between them, where nodes denote entities and ties represent a type of association between a pair of entities. This association can be friendship in social relations, a transaction in financial networks, or the possibility of infection in an epidemiological setting. While simple networks can represent the cooperation, alliance, friendship, communication, trust, and correlation between nodes, they lack the capability of incorporating the notion of rivalry, conflict, enmity, distrust, or negative correlation. Signed networks bring this possibility into a network model by introducing signed ties, with positive ties representing the former and negative ties representing the latter types of relations [1–3]. Therefore, signed networks have found many applications in various disciplines ranging from sociology [4–7], epidemiology [8], international relations [9–13], politics [14], and ecology [15].

Signed networks have been employed by the structural balance theory [16,17] to study the equilibrium states in networks with negative and positive associations. According to this theory, the state of balance for a network is defined based on the status of its triads, motifs consisting of three nodes with three ties connecting them. A *triad* is defined as balanced or nontensed if an even number of its ties are negative ([+, +, +], [−, −, +]). Otherwise, it is considered an unbalanced or tensed triad ([−, +, +], [−, −, −]) [16]. Intuitively, thinking of signs as friendship and enmity, it can be shown that balance holds when the following statements hold for all nodes in a triad:

(i) *The friend of my friend is my friend.* (ii) *The friend (enemy) of my enemy (friend) is my enemy.* (iii) *The enemy of my enemy is my friend.*

In the simplest versions of the model, tie signs get updated until the system reaches a fully balanced state. In this state, the network comprises two communities, where all intracommunity and intercommunity ties are respectively positive and negative. The classic works on the structural balance model dynamics are Refs. [18–20]. However, real-world social networks rarely arrive at a fully balanced state. While balanced triads are more prevalent, unbalanced triads still exist. To reflect this issue, a relaxed version of the theory has been devised by introducing a source of randomness and uncertainty via the adoption of the concept of the *social temperature* [21]. In other words, the systemic variable temperature accounts for a persistent form of disorder in the formation of the triadic relationships [22,23]. By doing so, the structural balance model has been mapped to a Boltzmann-Gibbs statistical model where each state is assigned with a probability $\frac{e^{-E/T}}{C}$. Here E denotes the system's energy in this state, T represents the social temperature, and C is the normalization factor. In this picture, the energy, $E_{\triangle}$, assigned to balanced and

*g_jafari@sbu.ac.ir

unbalanced triads, is respectively -1 and $+1$, so that states with a higher number of balanced triads are assigned with a high probability. T represents the level of tension tolerance in the system. With $T \to 0$, one would achieve the strict model in which only balanced triads are allowed, and $T \to \infty$ would lead to a system neutral toward triadic balanced/unbalanced.

The concept of temperature in socioeconomic systems has been widely contemplated [24–29]. Like the physical systems, the temperature is a measure of uncertainty and fluctuations in these systems. Let us consider the structural balance model as an example.

The structural balance model assigns a certain energy to any given configuration. If all agents update their dyadic relations to definitely minimize energy, then the temperature is zero [18]. As an example of interstate relations, the zero-temperature model suggests a bipolar world with two groups hostile toward each other. However, bipolarity does not happen often. Although countries try to eliminate tensions in triads they are involved in, there is also the potential of retaining some tensed triads due to different levels of tension tolerance. Hence, they do not restrict themselves to eliminating all tensed triads. If agents aim to minimize energy, but this is not their definite goal, then the system's behavior could be better modeled by the nonzero temperature balance model. To be more precise, triads with one or three hostile relations are considered tensed or unbalanced in structural balance, and the nonzero temperature model lets the system tolerate these tensed triplet interactions and makes the model more realistic.

In socioeconomic systems, agents are supposed to maximize utility function, minimize tension or energy function, etc. In some work, agents maximize utility with the Gibbs probability weight. In these works, a parameter is defined to control the chance of maximizing utility that is similar to the β factor in physical systems. If β is high, agents try to maximize utility as their major goal. As β decreases, then utility maximization happens with a moderate chance [25,26]. In summation, in socioeconomic systems, the temperature is a measure of uncertainty in the decision making.

Most analytical studies of the structural balance model have been conducted on complete graphs, neglecting the underlying network structures [21,30–34]. While empirical signed networks have also been employed [3,22,23], random networks have not attracted much attention in structural balance models. Random networks with controllable parameters have helped in understanding the effects of network characteristics on the dynamics of different phenomena such as spreading and percolation [35–37]. Hence, a similar methodology can be helpful in the study of the network aspects of the structural balance. Recently, the thermal behavior of structural balance has been investigated on diluted and enhanced triangular lattices by performing a series of simulations [38].

In this study, we first introduce a Hamiltonian for the structural balance model defined on a class of random graphs called Erdös-Rényi graphs. Then, we investigate the stationary states of our model in the presence of social temperature. We present a mean-field solution for our model under a canonical ensemble. We observe that the system undergoes a discontinuous phase transition by varying the temperature. We detect two transition temperatures which we name $T_{\rm cold}$ and $T_{\rm hot}$. For $T < T_{\rm cold}$ and $T > T_{\rm hot}$ the system would respectively settle in a completely balanced and a completely random phase. For $T_{\rm cold} < T < T_{\rm hot}$ the system undergoes a bistability phase experiencing both random and balanced phases. We calculate $T_{\rm cold}$ analytically and show that the coexistence region gets narrower as the connection probability decreases. Finally, we perform a series of Monte-Carlo simulations to support our mean-field solutions.

II. MODEL

This section presents a mean-field solution for the structural balance model defined on Erdös-Rényi networks. An Erdös-Rényi network is a static random network with a fixed number of nodes, in which each tie exists with an identical independent probability p [39].

Inspired by the structural balance Hamiltonian, we define the Hamiltonian of our model on Erdös-Rényi networks as

$$\mathbf{H} = -\frac{1}{N}\sum_{i<j<k} s_{ij}s_{jk}s_{ki}e_{ij}e_{jk}e_{ki}. \tag{1}$$

In Eq. (1), N is the number of nodes, and $s_{ij} \in \{+1, -1\}$ indicates the relationship between nodes i and j. Network topology is encoded in the adjacency matrix e, where $e_{ij} = 1$ if nodes i and j are connected, and $e_{ij} = 0$ otherwise. To evaluate the model, we need to investigate its observable macroscopic quantities. The macroscopic quantities in our model are ensemble averages of ties, two stars, and energy, respectively denoted by $\langle s_{ij}\rangle$, $\langle s_{ik}s_{kj}\rangle$, and $-\langle s_{ij}s_{jk}s_{ki}\rangle$. The role of the mean of two stars on the dynamic of thermal balance has been studied in Ref. [21]. This quantity measures the closeness of a network to the balanced state.

To calculate these quantities, we require the probability distribution of the possible states of the system. For this purpose, we define a partition function for our Hamiltonian (1) in a canonical ensemble of the s variable. The partition function is written as follows:

$$\mathbf{Z} = \sum_{\{\mathbf{s}\}} e^{-\beta\mathbf{H}}. \tag{2}$$

The $\{\mathbf{s}\}$ subscript indicates taking the summation over the ensemble of all possible signed ties in a static Erdös-Rényi network. Also $\beta = 1/T$ is defined as the inverse temperature in the Gibbs weight $e^{-\beta\mathbf{H}}$.

For evaluating statistical quantities using the Hamiltonian (1), we first assume that the graph configuration is fixed (quenched), and we sum over the link state variable $\mathbf{s} \equiv \{\mathbf{s_{ij}}\}$ for a given fixed set of $\mathbf{e_{ij}}$ generated by the probability distribution $P(e_{ij})$. For the free energy of the system, we have

$$F = -\frac{1}{\beta}\ln\mathbf{Z} = -\frac{1}{\beta}\ln\sum_{\{s_{ij}=\pm1\}} e^{-\beta H},$$

and hence the free energy is a function of $\mathbf{e} \equiv \{\mathbf{e_{ij}}\}$. In the next step, we average the free energy over an ensemble of Erdös-Rényi graph configurations to obtain the final expression of the free energy. The technique of averaging over all possible graph configurations is called *configurational averaging*. This averaging method is widespread in spin-glass literature [40].

We are allowed to first average over the link state variable and then over the configuration variable because the network configuration is fixed in the timescale of rapid fluctuations of the state of the links. The free energy obtained using this approach is called the *configurational free energy*, and we denote it by $[\mathbf{F}]_\mathbf{c} = -\frac{1}{\beta}[\ln \mathbf{Z}]_\mathbf{c}$. The $[\ ]_c$ represents the configurational averaging.

To calculate the ensemble average of a tie sign, $\langle s_{ij}\rangle$, we split the Hamiltonian into two parts [Eq. (3)], $\mathbf{H}_{ij}$ consisting of the terms which the tie $\{i, j\}$ contributes to (Eq. 4), and $\mathbf{H}'$ comprising the rest of the terms:

$$\mathbf{H} = \mathbf{H}_{ij} + \mathbf{H}', \tag{3}$$

$$\mathbf{H}_{ij} = -\frac{1}{N} s_{ij} \sum_{k\neq i,j} s_{jk}s_{ki}e_{jk}e_{ki} - h_{ij}s_{ij}, \tag{4}$$

where h_{ij} is considered as an external field on s_{ij}. Therefore, the partition function can be written as follows:

$$\begin{aligned}\mathbf{Z} &= \sum_{\{\mathbf{s}\}} e^{-\beta\mathbf{H}} = \sum_{\{\mathbf{s}\}} e^{-\beta(\mathbf{H}_{ij}+\mathbf{H}')} \\ &= \mathbf{Z}' \sum_{\{\mathbf{s}\neq s_{ij}\}} \frac{e^{-\beta\mathbf{H}'}}{\mathbf{Z}'} \sum_{s_{ij}=\{\pm 1\}} e^{-\beta\mathbf{H}_{ij}} = \mathbf{Z}'\left\langle \sum_{s_{ij}=\{\pm 1\}} e^{-\beta\mathbf{H}_{ij}} \right\rangle_{Z'} \\ &= \mathbf{Z}'\left\langle 2\cosh\left(\frac{\beta}{N}\sum_{k\neq i,j} s_{jk}s_{ki}e_{jk}e_{ki} + \beta h_{ij}\right)\right\rangle_{Z'} \\ &= 2\mathbf{Z}'\cosh\left(\frac{\beta}{N}\left\langle \sum_{k\neq i,j} s_{jk}s_{ki}e_{jk}e_{ki}\right\rangle_{Z'} + \beta h_{ij}\right).\end{aligned} \tag{5}$$

As a result of the mean-field approximation, the term $\langle \sum_{k\neq i,j} s_{jk}s_{ki}e_{jk}e_{ki}\rangle$ can be approximated by m, the number of triangles that two stars make with tie $\{i, j\}$, multiplied by the ensemble average of the two stars $\langle s_{jk}s_{ki}\rangle$. So we have

$$\mathbf{Z} = \mathbf{Z}_{ij}(m)\mathbf{Z}' = 2\cosh\left(\frac{\beta}{N} m\langle ss\rangle_{Z'} + \beta h_{ij}\right)\mathbf{Z}'. \tag{6}$$

Where we have decomposed the partition function into two parts $\mathbf{Z}_{ij}$ and $\mathbf{Z}'$, respectively, the parts which tie $\{i, j\}$ do and do not contribute. From statistical mechanics we have [21]

$$\langle s_{ij}\rangle = -\frac{\partial[\mathbf{F}]_c}{\partial h_{ij}}\bigg|_{h_{ij}=0}. \tag{7}$$

So, we have to calculate the *configurational free energy* $[\mathbf{F}]_c$, Where $[\ ]_c$ indicates the integral over all possible random graph configurations. As we can split the partition function in the form of $\mathbf{Z} = \mathbf{Z}_{ij}\mathbf{Z}'$, we can write the *configurational free energy* as a sum of two terms, in which the first term represents the integration of the partition function $\mathbf{Z}_{ij}$ over the terms including tie $\{i, j\}$ and the second term represents the integration of the partition function $\mathbf{Z}'$ over the rest. Therefore, we have

$$\begin{aligned}[\mathbf{F}]_c &= -\frac{1}{\beta}\left([\mathbf{F}']_{c'} + \sum_{c_{ij}} \ln \mathbf{Z}_{ij}\right) \\ &= -\frac{1}{\beta}\left([\mathbf{F}']_{c'} + \sum_{m}^{N-2} P(m)\ln \mathbf{Z}_{ij}(m)\right).\end{aligned} \tag{8}$$

The details of the calculation can be found in Appendix A. The first term of Eq. (8) does not play a role in our calculations, so we can consider it a constant.

As Eq. (6) indicates, $\mathbf{Z}_{ij}$ is a function of m, the number of triangles including the tie $\{i, j\}$, so the second term can be approximated by a summation over values of m. Defining $P(m)$ the probability of generation of m triangles, including the tie $\{i, j\}$, we have

$$P(m) = \binom{N-2}{m}(p^2)^m[(1-p)^2 + 2p(1-p)]^{N-2-m}. \tag{9}$$

Therefore, $[\mathbf{F}]_c$ will be

$$[\mathbf{F}]_c = -\frac{[\mathbf{F}']_{c'}}{\beta} - \frac{1}{\beta}\ln\left[\cosh\left(\frac{\beta}{N}(N-2)p^2\langle ss\rangle_{\mathbf{Z}'} + \beta h_{ij}\right)\right]. \tag{10}$$

In Eq. (10) we have used $\sum_{m=0}^{N-2} mP(m) = (N-2)p^2$ which is the first moment of the binomial distribution. For $\langle s_{ij}\rangle$ we have

$$\begin{aligned}\langle s_{ij}\rangle &= -\frac{\partial[\mathbf{F}]_c}{\partial h_{ij}}\bigg|_{h_{ij}=0} \\ &= -\frac{\partial[\mathbf{F}']_{c'}}{\partial h_{ij}}\bigg|_{h_{ij}=0} \\ &\quad + \frac{1}{\beta}\frac{\partial}{\partial h_{ij}}\ln\left[\cosh\left(\frac{\beta}{N}(N-2)p^2\langle ss\rangle_{Z'} + \beta h_{ij}\right)\right]\bigg|_{h_{ij}=0} \\ &= 0 + \tanh\left(\frac{\beta}{N}(N-2)p^2\langle ss\rangle_{Z'} + \beta h_{ij}\right)\bigg|_{h_{ij}=0}\end{aligned}$$

So, the average of signed edges, $\langle s\rangle$, is

$$\langle s\rangle = \tanh\left(\beta p^2\frac{N-2}{N}\langle ss\rangle\right). \tag{11}$$

As Eq. (11) indicates, $\langle s\rangle$ is a function of the ensemble average of two stars, $\langle ss\rangle$. To calculate $\langle ss\rangle$, we employ a similar method, where we split the Hamiltonian into $\mathbf{H}_{jk,ki}$ and $\mathbf{H}''$. The first term comprises the terms including at least one of the ties $\{i, k\}$ and $\{k, j\}$, [Eq. (12)] and the second term comprises the rest:

$$\begin{aligned}\mathbf{H}_{ik,kj} = &-\frac{1}{N}s_{ik}\sum_{l\neq i,j,k} s_{il}s_{lk}e_{il}e_{lk} - \frac{1}{N}s_{kj}\sum_{l\neq i,j,k} s_{kl}s_{lj}e_{kl}e_{lj} \\ &- \frac{1}{N}s_{ik}s_{kj}s_{ij} - s_{ik}s_{kj}h_{ik,kj},\end{aligned} \tag{12}$$

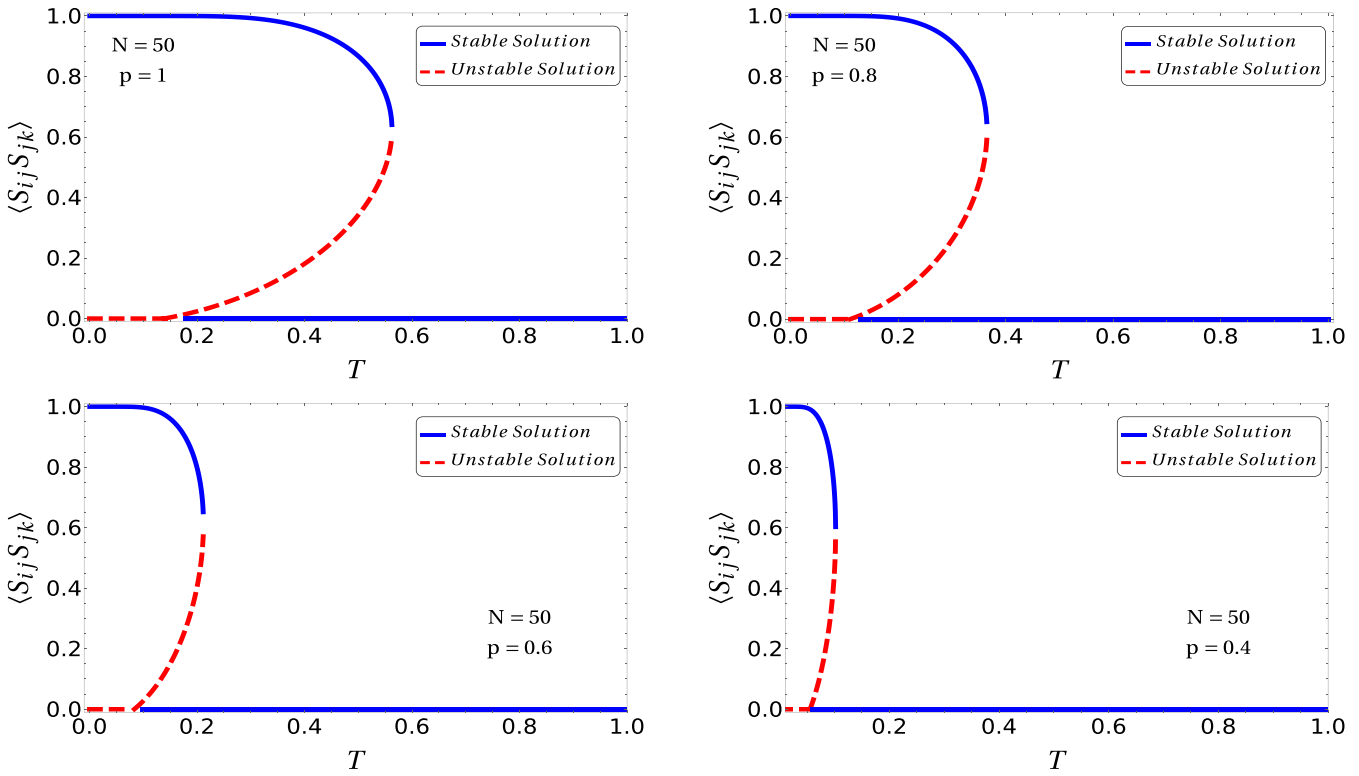

FIG. 1. "Blue-sky" bifurcation diagram versus temperature for an Erdös-Rényi random graph with $N = 50$ nodes and four connection probabilities $p = 1$, $p = 0.8$, $p = 0.6$, and $p = 0.4$ in the mean-field approximation. For each p, three distinct regions are observed. The random graph is in the balanced phase for $T < T_{\text{cold}}$. It is completely in a random phase for $T > T_{\text{hot}}$. For $T_{\text{cold}} < T < T_{\text{hot}}$, the random network experiences the coexistence phase.

where $h_{ik,kj}$ is considered as an external field on two stars $s_{ik}s_{kj}$. The partition function can be written as follows:

$$\begin{aligned}\mathbf{Z} &= \sum_{\{\mathbf{s}\}} e^{-\beta\mathbf{H}} = \sum_{\{\mathbf{s}\}} e^{-\beta(\mathbf{H}_{ik,kj}+\mathbf{H}'')} \\ &= \mathbf{Z}'' \sum_{s\neq s_{ik},s_{kj}} \frac{e^{-\beta\mathbf{H}''}}{\mathbf{Z}''} \sum_{s_{ik}=\pm1} \sum_{s_{kj}=\pm1} e^{-\beta\mathbf{H}_{ik,kj}} \\ &= \mathbf{Z}'' \left\langle \sum_{s_{ik}=\pm1} \sum_{s_{kj}=\pm1} e^{-\beta\mathbf{H}_{ik,kj}} \right\rangle_{Z''}. \end{aligned} \tag{13}$$

Substituting Eq. (12) in Eq. (13), we have

$$\begin{aligned}\mathbf{Z} = \mathbf{Z}''\big(&e^{\frac{\beta}{N}(m_1\langle s_{il}s_{lk}\rangle_{Z''}+m_2\langle s_{kl}s_{lj}\rangle_{Z''}+\langle s_{ij}\rangle_{Z''})+\beta h_{ik,kj}} \\ &+ e^{\frac{\beta}{N}(m_1\langle s_{il}s_{lk}\rangle_{Z''}-m_2\langle s_{kl}s_{lj}\rangle_{Z''}-\langle s_{ij}\rangle_{Z''})-\beta h_{ik,kj}} \\ &+ e^{\frac{\beta}{N}(-m_1\langle s_{il}s_{lk}\rangle_{Z''}+m_2\langle s_{kl}s_{lj}\rangle_{Z''}-\langle s_{ij}\rangle_{Z''})-\beta h_{ik,kj}} \\ &+ e^{\frac{\beta}{N}(-m_1\langle s_{il}s_{lk}\rangle_{Z''}-m_2\langle s_{kl}s_{lj}\rangle_{Z''}+\langle s_{ij}\rangle_{Z''})+\beta h_{ik,kj}}\big), \end{aligned} \tag{14}$$

where m_1 and m_2 are the number of triangles established on ties $\{i, k\}$ and $\{k, j\}$, respectively, not including nodes j and i.

The homogeneity of the Erdös-Rényi random graph allows us to assume $m_1 = m_2$. From statistical mechanics, we have [21]

$$\langle s_{ik}s_{kj}\rangle = -\frac{\partial[\mathbf{F}]_c}{\partial h_{ik,kj}}\bigg|_{h_{ik,kj}=0}. \tag{15}$$

So, for the mean of two stars we have

$$\langle ss\rangle = \frac{\left(e^{\beta(2p^2\frac{N-3}{N}\langle ss\rangle)} - 2e^{\beta(-2\frac{\langle s\rangle}{N})} + e^{\beta(-2p^2\frac{N-3}{N}\langle ss\rangle)}\right)}{\left(e^{\beta(2\frac{N-3}{N}p^2\langle ss\rangle)} + 2e^{\beta(-2\frac{\langle s\rangle}{N})} + e^{\beta(-2p^2\frac{N-3}{N}\langle ss\rangle)}\right)}. \tag{16}$$

Details of this calculation are given in Appendix B. By replacing Eq. (11) in Eq. (16) we reach a self-consistent equation that yields the ensemble average of the two stars for any temperature T, based on the connection probability p and the network size N. The intersections of Eq. (16) yield its fixed points. We illustrate this result for different p values in Appendix D. Figure 1 depicts the bifurcation diagram versus temperature for different connection probabilities in an Erdös-Rényi graph of size N. As shown in Fig. 1, the bifurcation is of the "blue-sky" type, which is the characteristic of a discontinuous phase transition which leads to three distinct regions.

(i) For $T > T_{\text{hot}}$ or the high-temperature regime, there exists one stable fixed point with $q^* = 0$. From an intuitive point of view, $q^* = 0$ refers to the society that is in a random phase, where the number of balanced and unbalanced triads are equal and large thermal fluctuations prevent the formation of any structural balance in the network. In other words, in this condition, balanced triads have no superiority over unbalanced triads.

(ii) For $T_{\text{cold}} < T < T_{\text{hot}}$ or the coexistence region, there exist three fixed points of which two are stable ($q_1^* = 0, q_2^*$) and the other one is unstable. Since we have two

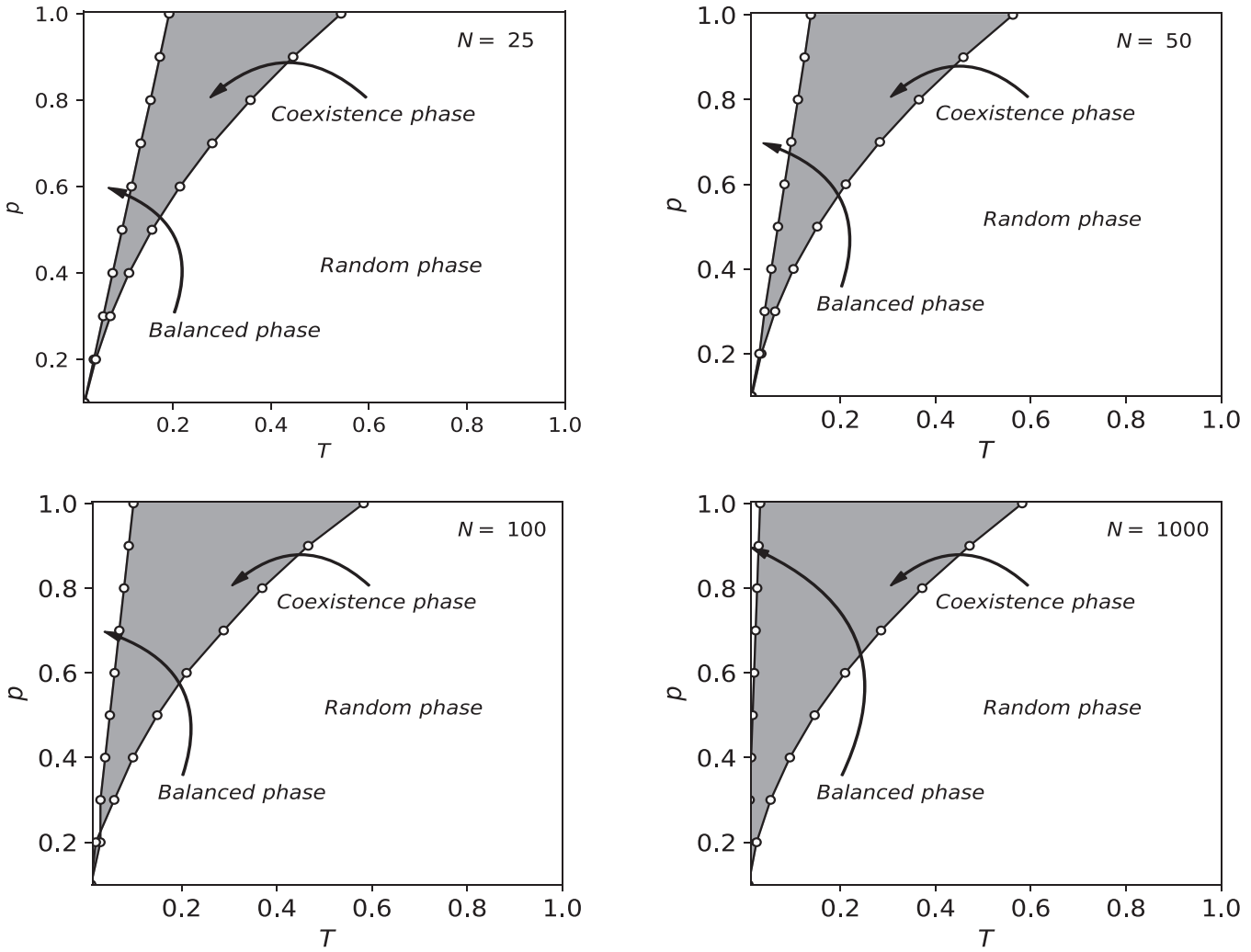

FIG. 2. The phase diagram in (T, p) space for Erdös-Rényi random graphs with $N = 25$, 50, 100, and 1000 nodes, respectively. As indicated, the shaded region represents the coexistence phase in which random and balanced phases coexist.

stable fixed points in this region, the system experiences the coexistence of both random and balanced phases. The hysteresis loop is obtained due to the coexistence of balanced and random phases within a specified temperature range.

(iii) For $T < T_{\text{cold}}$ or the low-temperature regime, there exist two fixed points with $q_1^* = 0$ and $q_2^* = 1$. The first one is an unstable fixed point, and the second one is stable. From an intuitive point of view, a signed order is formed when the temperature is low enough, and the system is in a balanced phase. In other words, tie signs are frozen because of a strong two-star field $q^* = 1$.

As it is shown for the blue-sky bifurcation diagram in Fig. 1, the cold critical temperature T_{cold} is where the coexistence region starts appearing. To derive this point analytically, we need to take the first derivative of the self-consistent Eq. (16) with respect to q: As we know from stability analysis, the fixed points of a self-consistent equation $f(q^*) = q^*$ are stable if $f'(q^*) < 1$ and unstable if $f'(q^*) > 1$. Thus, $q^* = 0$ is stable when $f'(q^* = 0) = \beta^2 p^2 (\frac{N-2}{N^2}) < 1$. Therefore we have

$$T_{\text{cold}} = p\sqrt{\frac{N-2}{N^2}}. \tag{17}$$

Hence, the cold critical temperature has a linear dependency on the connection probability p. Furthermore, the cold critical temperature converges to zero in the limit of large N values. This leads to the vanishing of the purely balanced phase even for low temperatures.

In Fig. 2 we have illustrated the phase diagram of the ensemble average of the two stars as a function of p and T to analyze the behavior of the coexistence region in the (p, T) phase space. Figure 2 indicates the phase diagram in the (p, T) space for an Erdös-Rényi random graph with the connection probability p at temperature T for network sizes $N = 25$, 50, 100, and 1000. As it is shown, the phase space is divided into three regions. The shaded region represents the p and T values leading to a bistability in the system, in which both random and balanced phases coexist. As illustrated, an increase in the size of the random graph enlarges the coexistence region and

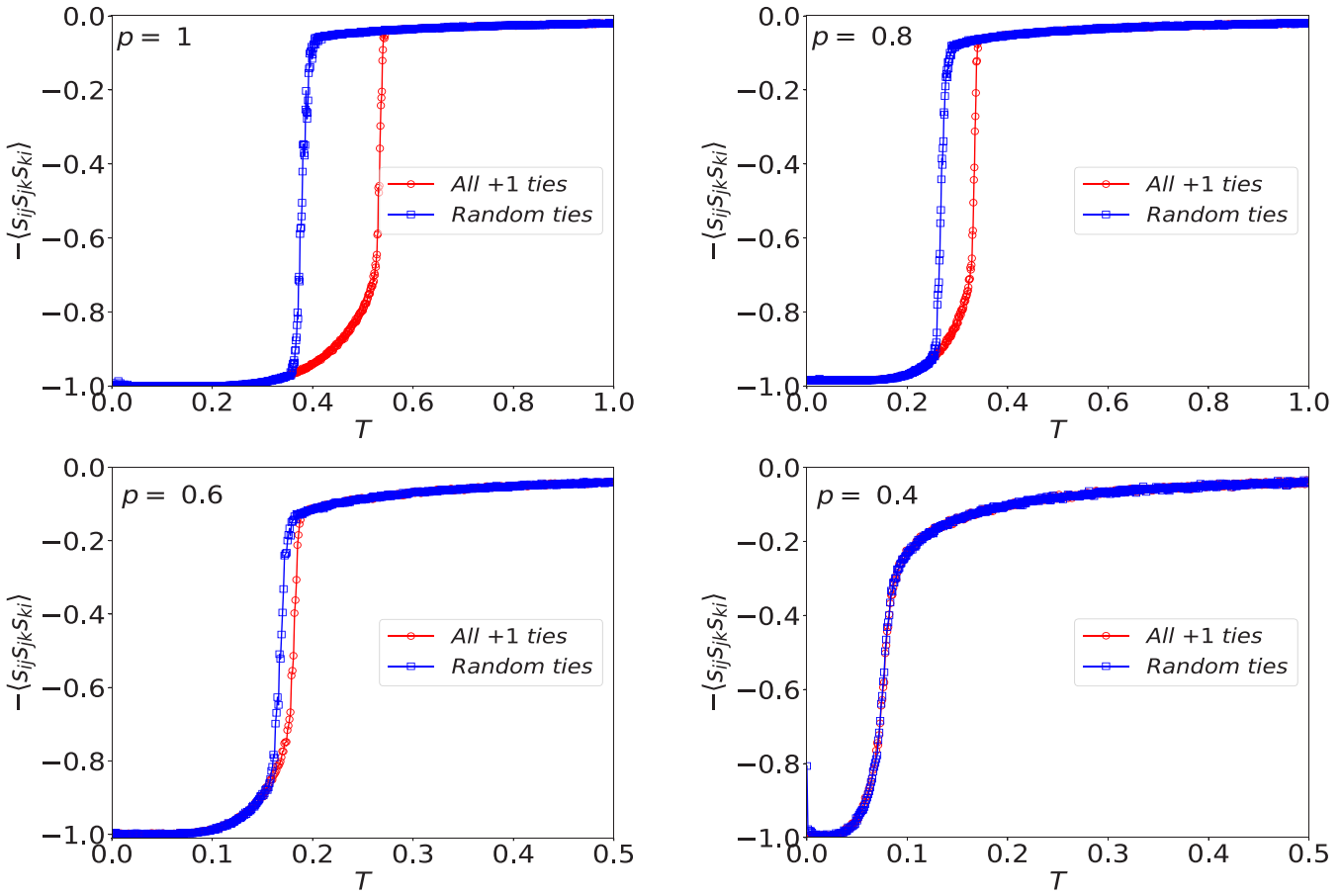

FIG. 3. The mean of energy versus temperature for four connection probabilities, $p = 1$, $p = 0.8$, $p = 0.6$, and $p = 0.4$, in an Erdös-Rényi Random graph of size $N = 50$. As it is apparent, with increasing the network sparsity, both T_{hot} and T_{cold} decrease, but the slope of decreasing T_{hot} is more than the slope of decreasing T_{cold}. Therefore, the coexistence region totally vanishes by reaching a specific value of connection probability.

decreases T_{cold}, so that for sufficiently large sizes the pure balance phase vanishes.

In the next section, we verify our mean-field solution by a series of Monte-Carlo simulations.

III. SIMULATION

We generate 1000 realizations of an Erdös-Rényi random graph with size $N = 50$ and the connection probability p. Each tie is initially in the $(+)$ state with the probability α and in the $(-)$ state with the probability $1 - \alpha$. We consider two different initial conditions: (i) $\alpha = 1$ (all $+$ 1), and (ii) $\alpha = 0.5$ (random signs). To reach a stationary state of the system, we apply a Metropolis-Hastings algorithm on the tie signs with N^3 Monte Carlo steps. The algorithm is as follows.

(i) We choose a random tie and consider flipping its sign. If the energy variation is negative, i.e., $\Delta\mathbf{E} = \mathbf{E}_f - \mathbf{E}_i < 0$, the flip is accepted. Where E_i and E_f indicate the system's energy before and after the flip.

(ii) If the energy variation is semipositive, i.e., $\Delta\mathbf{E} = \mathbf{E}_f - \mathbf{E}_i \geqslant 0$, the flip is accepted with the Boltzmann probability $e^{-\Delta\mathbf{E}/\mathbf{T}}$.

(iii) This procedure continues for N^3 Monte Carlo steps to reach the stationary state.

Figure 3 illustrates the average energy, $\langle\mathbf{E}\rangle = -\langle s_{ij}s_{jk}s_{ki}\rangle$, versus temperature for different connection probabilities. We observe two curves, each corresponding to an initial condition: the curve obtained for the random initial condition has a critical point at $T = T_{\text{cold}}$, and the curve obtained for the all $+$ 1 initial condition has a critical point at $T = T_{\text{hot}}$. Therefore, simulation results correctly capture the two critical temperatures T_{cold} and T_{hot}.

Furthermore, By decreasing the connection probability p, the coexistence region becomes narrower until it completely vanishes in $p \approx 0.4$. In addition, the hot critical temperature T_{hot} is in good agreement with the mean-field solution.

On the other hand, since the basin of attraction of $q^* = 0$ in the coexistence region is very narrow, it is practically challenging to capture T_{cold} via the simulation for all temperatures.

IV. CONCLUSION

The idea of standard balance on empirical data obtained from real signed networks has brought the opportunity to capture exciting phenomena in political networks, psychology, international relations, and ecology. However, little has been done so far to investigate signed random networks with an analytical approach. On the other hand, the idea of eliminating tension in all triadic relationships in signed networks inspired

by structural balance theory does not come true for many signed networks. For instance, in social networks, agents may tend to change their relations with the other agents, even though these changes are not in favor of total tension reduction. Thus, the concept of social temperature has been introduced to capture different levels of tension tolerance [21]. Therefore, there is a competition between agents' random behavior (social temperature) and the tendency to reach a state of balance. Considering these two issues, we have proposed a model that defines the structural balance on Erdös-Rényi networks in the presence of temperature within a theoretical framework.

We have solved the model with a mean-field approach. We have detected a discontinuous phase transition with temperature. We have captured two temperatures, $T_{\rm cold}$ and $T_{\rm hot}$, which lead to three distinct regions: For $T < T_{\rm cold}$, the system is in a completely balanced phase. On the other hand, for $T > T_{\rm hot}$, the system cannot reach the balanced phase. For $T_{\rm cold} < T < T_{\rm hot}$, the system demonstrates bistability with two stable fixed points $q_1^* = 0$ and q_2^* respectively denoting the random and balanced phases. Regarding the bistability region, the system experiences a hysteresis phenomenon. Hence, depending on the initial condition, the system meets one of the two curves surrounding the coexistence region. Therefore, we do not need to overcool the system to enter the bipolar state. The system enters the bipolar state even for moderate temperatures. Another outcome of the model is the following: the less the connection probability is, the closer $T_{\rm cold}$ and $T_{\rm hot}$ become. Solving $T_{\rm cold}$ analytically, we derive that for large Erdös-Rényi networks $T_{\rm cold}$ converges to 0. Counterintuitively, this indicates that even for $T \approx 0$ the system can be in a random state.

The social consequences of this phase transition and the hysteresis phenomena would be as follows. Let us imagine a society where the level of tension tolerance is high ($T > T_{\rm hot}$). Hence, this condition has no structural balance, and the society is in a random state. In this state, balanced triads have no superiority over unbalanced triads. Imagine that tension tolerance decreases due to conflict, the political bargaining, access to resources, trading partners, etc. Different scenarios may happen depending on how much the tension tolerance is reduced.

(a) If the tension tolerance drops sharply (from $T > T_{\rm hot}$ to $T < T_{\rm cold}$), the society is immediately divided into two mutually hostile groups. Hence, the fate of a society with low tension tolerance would be a bipolar state, as we would expect intuitively. For instance, in a politically polarized society, people cannot positively bond with other people from the opposite party.

(b) If the tension tolerance decreases moderately (from $T > T_{\rm hot}$ to $T_{\rm cold} < T < T_{\rm hot}$), the society may stay at its random state with no structural balance. However, this random state has fragile stability, so a small perturbation can take society out of its random state into a bipolar state, although the tension tolerance is still above the $T_{\rm cold}$ (bistability phenomenon).

(c) If a small perturbation takes the society out of its random state into a bipolar state ($T_{\rm cold} < T < T_{\rm hot}$), then it would not be possible to take it out of its polarized state unless the level of tension tolerance exceeded the critical point ($T > T_{\rm hot}$). In other words, raising the level of tension tolerance up to the initial point is not sufficient to return the society to the random state (hysteresis phenomena). This has a crucial consequence from the sociological point of view; if we want to take society out of its polarized phase, the practical solution is to raise the level of tension tolerance in society at least up to the $T_{\rm hot}$, instead of engineering relationships between people.

We spanned the phase space (T, p) to analyze the coexistence region. We observed that by reaching a specific value of connection probability the coexistence region vanishes. We have conducted a series of Monte Carlo simulations to verify the result we obtained by the mean-field approach. There is a good agreement for the behavior of the hot temperature between the two approaches. The minor discrepancy for the cold temperature in the two approaches is due to the fact that the basin of attraction of $q^* = 0$ is narrow and hard to completely capture in a Monte Carlo simulation.

APPENDIX A: CONFIGURATIONAL FREE ENERGY: ONE-BODY HAMILTONIAN APPROACH

For calculating the *configurational free energy*, we have to take the configurational average of the *quenched partition function* over all possible random graph configurations. Therefore we have

$$\begin{aligned}
[\mathbf{F}]_c &= -\frac{1}{\beta}[\ln \mathbf{Z}]_c = -\frac{1}{\beta}[\ln(\mathbf{Z}_{ij}\mathbf{Z}')]_c = -\frac{1}{\beta}[\ln \mathbf{Z}' + \ln \mathbf{Z}_{ij}]_c \\
&= -\frac{1}{\beta}[\ln \mathbf{Z}']_c - \frac{1}{\beta}[\ln \mathbf{Z}_{ij}]_c \\
&= -\frac{1}{\beta}[[\ln \mathbf{Z}']_{c_{ij}}]_{c'} - \frac{1}{\beta}[[\ln \mathbf{Z}_{ij}]_{c'}]_{c_{ij}} \\
&= -\frac{1}{\beta}[\ln \mathbf{Z}']_{c'} - \frac{1}{\beta}[\ln \mathbf{Z}_{ij}]_{c_{ij}} \\
&= -\frac{1}{\beta}([\mathbf{F}']_{c'} + [\mathbf{F}_{ij}]_{c_{ij}}). \qquad \text{(A1)}
\end{aligned}$$

In Eq. (A1), the bracket $[\ ]_c$ indicates the configurational average of partition function over all possible random graph configurations. As we explained in the model section, we can decompose the partition function to two parts, $\mathbf{Z}_{ij}$ and $\mathbf{Z}'$, that existing tie $\{i, j\}$ does and does not contribute to. Therefore, we can write the configurational free energy as the sum of two terms: the first term of Eq. (A1), $-\frac{1}{\beta}[\mathbf{F}']_{c'}$, does not play a role in our calculations, so we can take it as a constant. From Eq. (5), we know that $\mathbf{Z}_{ij}$ for a quenched configuration is a function of $\langle \sum_k s_{jk}s_{ki}e_{jk}e_{ki}\rangle_{Z'}$. We make an approximation in this step and suppose that the abovementioned quantity that appears in $\mathbf{Z}_{ij}$ is approximated by the number of triangles, i.e., m established on existing tie $\{i, j\}$, multiplied by the mean of two stars, i.e., $\langle ss\rangle$, in that specific quenched configuration. So in Eq. (A1) the sum over $\{c_{ij}\}$ is approximated by the sum over all possible numbers of triangles (m) multiplied by the probability of establishing m triangles on the tie $\{i, j\}$, i.e., $P(m)$.

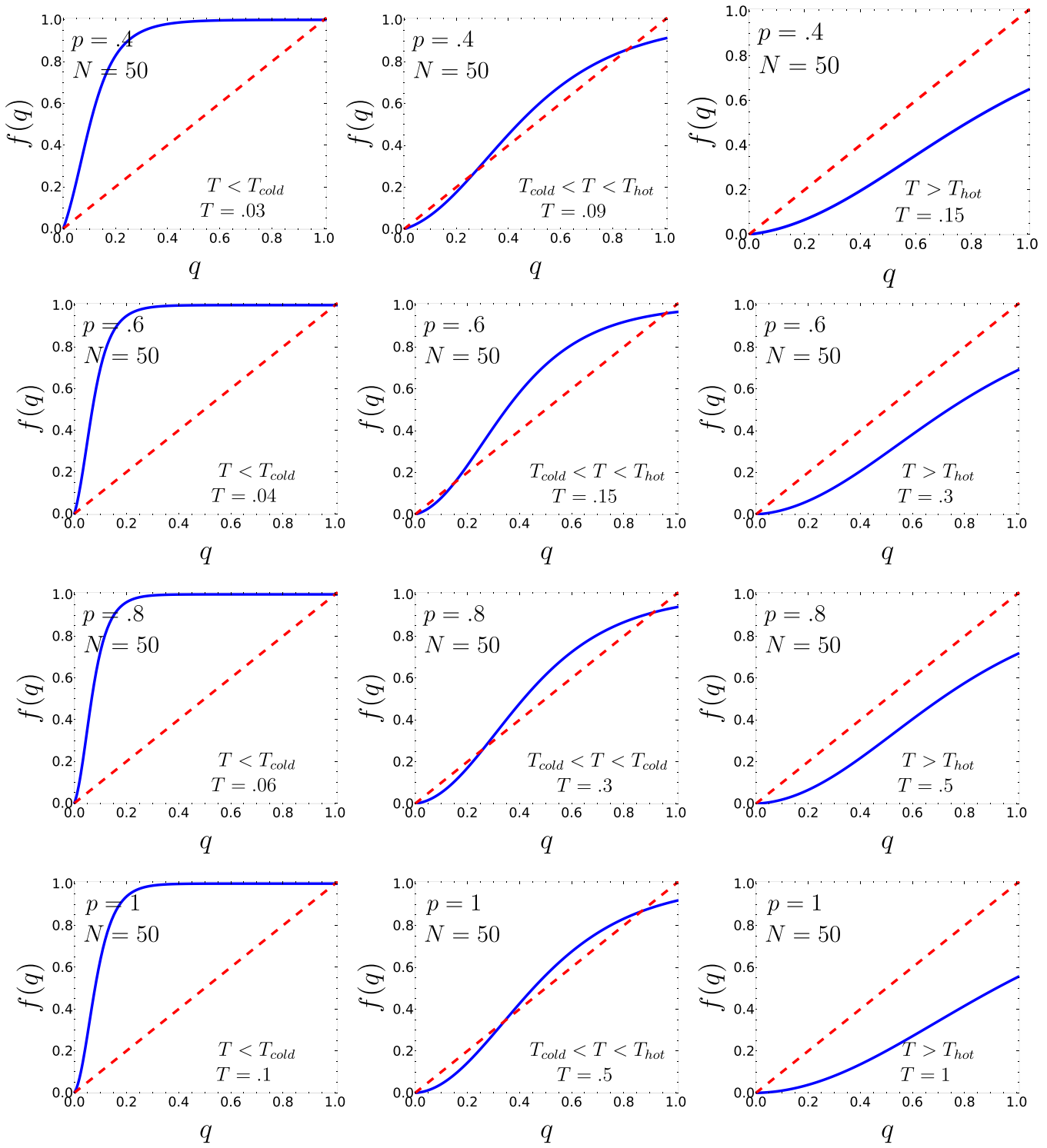

FIG. 4. Graphical representation of self-consistent Eq. (16) for four connection probabilities, $p = 1$, $p = 0.8$, $p = 0.6$, and $p = 0.4$, in three distinct phases for an Erdös-Rényi network with $N = 50$ nodes.

So we have

$$[\mathbf{F}]_c = -\frac{1}{\beta}\left([\mathbf{F}']_{c'} + \sum_{m=0}^{N-2} P(m) \ln \mathbf{Z}_{ij}(m)\right) = -\frac{1}{\beta}\left\{[\mathbf{F}']_{c'} + \sum_{m=0}^{N-2} P(m) \ln\left[\cosh\left(\frac{\beta}{N} m\langle ss\rangle_{Z'} + \beta h_{ij}\right)\right]\right\}. \tag{A2}$$

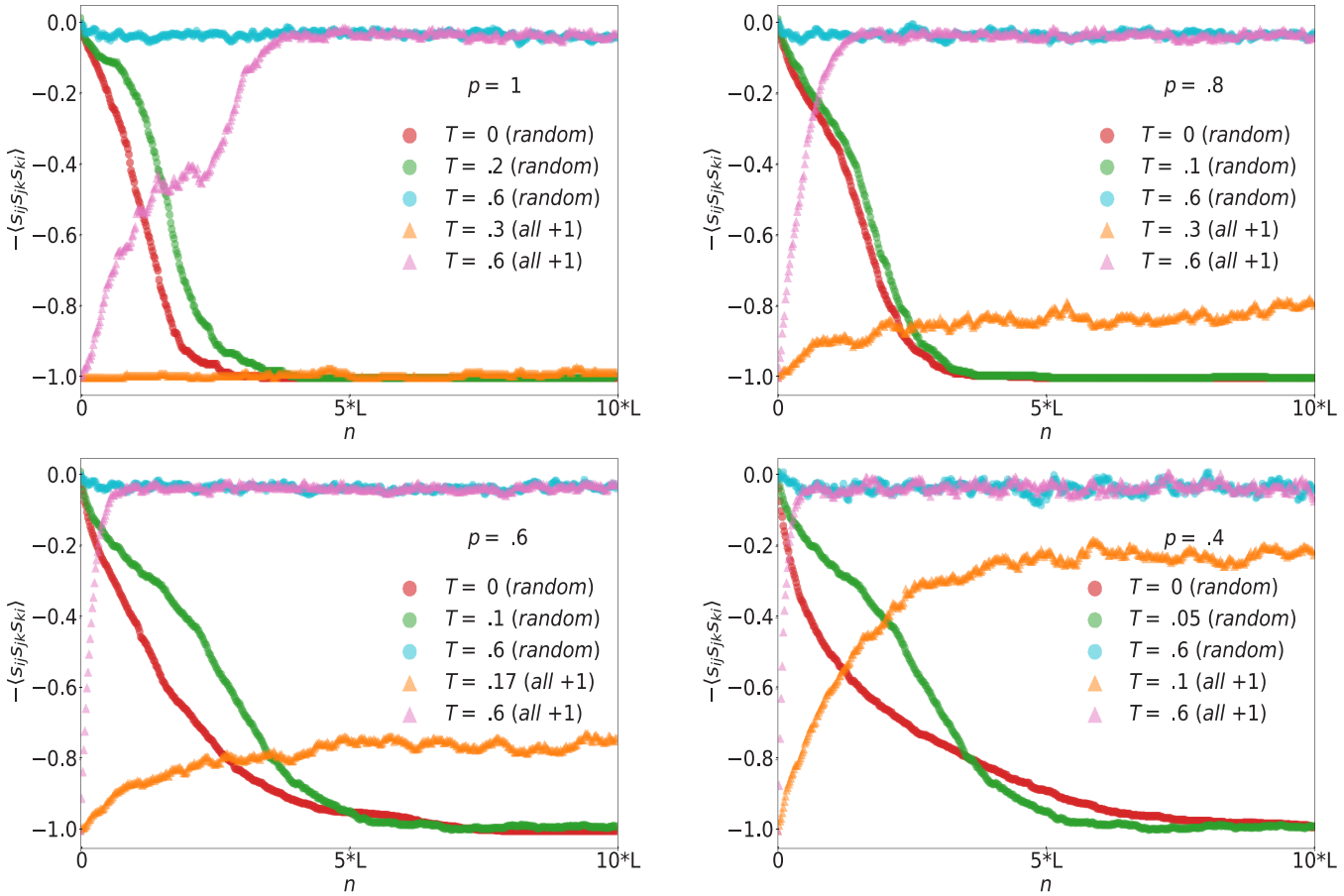

FIG. 5. Mean of energy during the evolution of an Erdös-Rényi random network with $N = 50$ nodes and connection probabilities $p = 1$, 0.8, 0.6, and 0.4 for a single trial with two different initial conditions, random and all + 1, in different temperatures.

APPENDIX B: CONFIGURATIONAL FREE ENERGY: TWO-BODY HAMILTONIAN APPROACH

Like the approach we applied for calculating the *configurational free energy* regarding the one-body Hamiltonian partition function, for calculating the *configurational free energy* of the system regarding the two-body Hamiltonian partition function, we separate the $\{ik, kj\}$ part and follow a similar procedure. Therefore we have

$$
\begin{aligned}
[\mathbf{F}]_c &= -\frac{1}{\beta}\left([\mathbf{F}'']_{c''} + \sum_{\{c_{ik,kj}\}} \ln \mathbf{Z}_{ik,kj}\right) \\
&= -\frac{[\mathbf{F}'']_{c''}}{\beta} - \frac{1}{\beta}\sum_{m_1=0}^{N-3}\sum_{m_2=0}^{N-3} P(m_1)P(m_2)\ln[\mathbf{Z}_{ik,kj}(m_1,m_2)] \\
&= -\frac{[\mathbf{F}'']_{c''}}{\beta} - \frac{1}{\beta}\sum_{m_1=0}^{N-3}\sum_{m_2=0}^{N-3} P(m_1)P(m_2)\ln\Big[e^{\frac{\beta}{N}(m_1\langle s_{il}s_{lk}\rangle_{Z'}+m_2\langle s_{kl}s_{lj}\rangle_{Z''}+\langle s_{ij}\rangle_{Z''})+\beta h_{ik,kj}} \\
&\quad + e^{\frac{\beta}{N}(m_1\langle s_{il}s_{lk}\rangle_{Z''}-m_2\langle s_{kl}s_{lj}\rangle_{Z''}-\langle s_{ij}\rangle_{Z''})-\beta h_{ik,kj}} + e^{\frac{\beta}{N}(-m_1\langle s_{il}s_{lk}\rangle_{Z''}+m_2\langle s_{kl}s_{lj}\rangle_{Z''}-\langle s_{ij}\rangle_{Z''})-\beta h_{ik,kj}} \\
&\quad + e^{\frac{\beta}{N}(-m_1\langle s_{il}s_{lk}\rangle_{Z''}-m_2\langle s_{kl}s_{lj}\rangle_{Z''}+\langle s_{ij}\rangle_{Z''})+\beta h_{ik,kj}}\Big] \\
&= -\frac{[\mathbf{F}'']_{c''}}{\beta} - \frac{1}{\beta}\ln\Big[e^{\beta(2p^2\frac{(N-3)}{N}\langle ss\rangle+\frac{\langle s\rangle}{N}+h_{ik,kj})} + 2e^{\beta(\frac{-\langle s\rangle}{N}-h_{ik,kj})} + e^{\beta(-2p^2\frac{(N-3)}{N}\langle ss\rangle+\frac{\langle s\rangle}{N}+h_{ik,kj})}\Big],
\end{aligned}
\tag{B1}
$$

where m_1 and m_2 are the number of triangles established on ties $\{i, k\}$ and $\{k, j\}$, respectively, not including nodes j and i. The homogeneity of the Erdös-Rényi random graph lets us assume $m_1 = m_2$. From statistical mechanics we know that the mean of

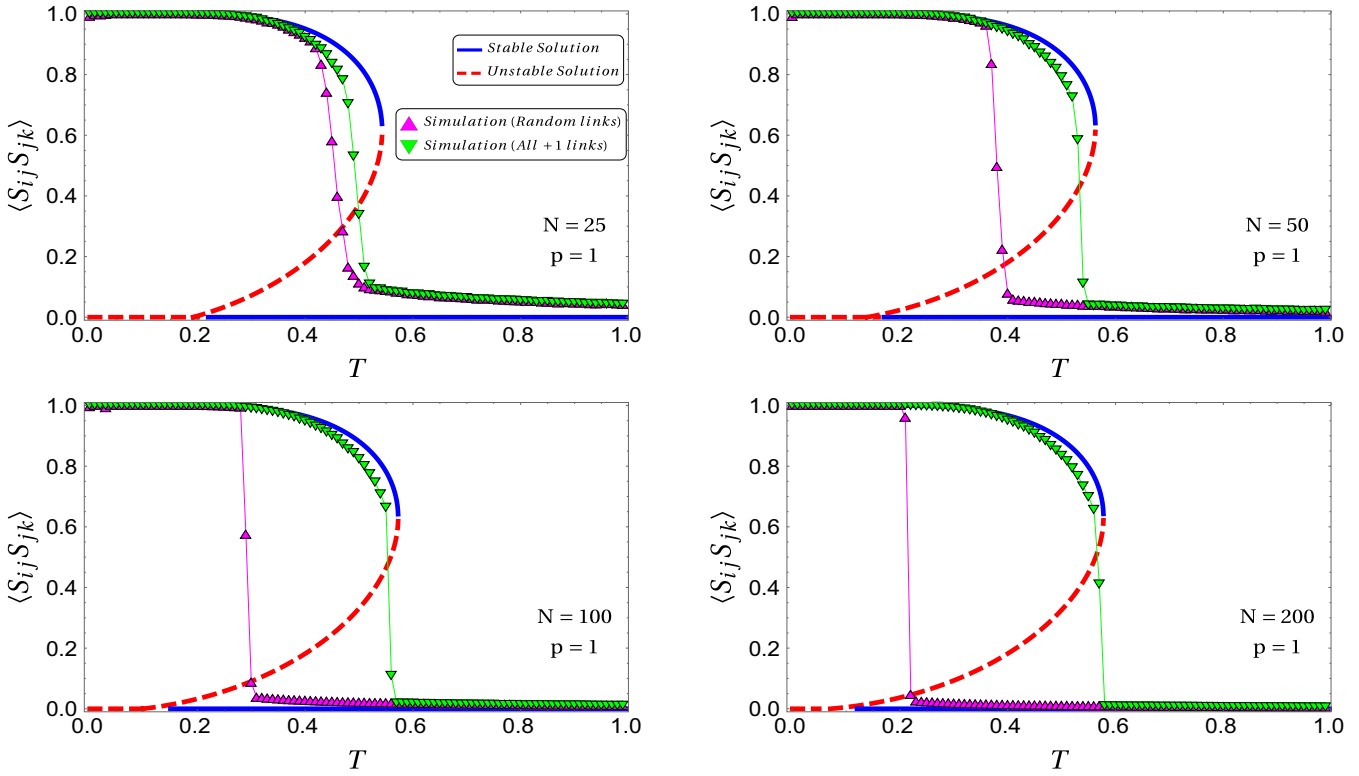

FIG. 6. Compatibility between Monte Carlo simulation (triangle-line curves) and mean-field solution (blue solid and red dashed curves) for the mean of two stars versus temperature. We have considered four Erdös-Rényi random networks with $N = 25$, 50, 100, and 200 nodes with the connection probability $p = 1$.

two stars, $\langle s_{ik}s_{kj}\rangle$, is the first derivative of free energy with respect to the field $h_{ik,kj}$:

$$\begin{aligned}\langle s_{ik}s_{kj}\rangle &= -\frac{\partial[\mathbf{F}]}{\partial h_{ik,kj}}\bigg|_{h_{ik,kj}=0}\\ &= -\frac{\partial\big(-\frac{[\mathbf{F}'']_{c''}}{\beta}\big)}{\partial h_{ik,kj}}\bigg|_{h_{ik,kj}=0} + \frac{1}{\beta}\frac{\partial}{\partial h_{ik,kj}}\ln\Big[e^{\beta(2p^2\frac{(N-3)}{N}\langle ss\rangle+\frac{\langle s\rangle}{N}+h_{ik,kj})} + 2e^{\beta(\frac{-\langle s\rangle}{N}-h_{ik,kj})} + e^{\beta(-2p^2\frac{(N-3)}{N}\langle ss\rangle+\frac{\langle s\rangle}{N}+h_{ik,kj})}\Big]\bigg|_{h_{ik,kj}=0}\\ &= 0 + \frac{\big(e^{\beta(2p^2\frac{N-3}{N}\langle ss\rangle)} - 2e^{\beta(-2\frac{\langle s\rangle}{N})} + e^{\beta(-2p^2\frac{N-3}{N}\langle ss\rangle)}\big)}{\big(e^{\beta(2\frac{N-3}{N}p^2\langle ss\rangle)} + 2e^{\beta(-2\frac{\langle s\rangle}{N})} + e^{\beta(-2p^2\frac{N-3}{N}\langle ss\rangle)}\big)}.\end{aligned} \tag{B2}$$

APPENDIX C: CALCULATING COLD CRITICAL TEMPERATURE

As we discussed earlier, $T_{\rm cold}$ is where the coexistence region starts appearing. We know that in the coexistence region $q^* = 0$ is a stable fixed point. Hence, for calculating $T_{\rm cold}$, we need to drive the first derivative of the right-hand side of the self-consistent equation $q = f(q)$ in $q^* = 0$. We need to have it as a stable fixed point so we should have $f'(q^* = 0) < 1$. Therefore we have

$$\begin{aligned}&\frac{\partial f(q)}{\partial q}\bigg|_{q=0}\\ &= \frac{\big(4\beta p^2\big(\frac{N-3}{N}\big)\sinh\big[2\beta p^2\big(\frac{N-3}{N}\big)q\big] + 4\beta^2p^2\big(\frac{N-2}{N^2}\big)\big\{1-\tanh^2\big[\beta p^2\big(\frac{N-2}{N}\big)q\big]\big\}e^{-2\beta\frac{\langle s\rangle}{N}}\big)\big(2\cosh\big[2\big(\frac{N-3}{N}\big)\beta p^2q\big] + 2e^{-2\beta\langle s\rangle}\big)}{\big(2\cosh\big[2\beta p^2\frac{N-3}{N}q\big] + 2e^{-2\beta\frac{\langle s\rangle}{N}}\big)^2}\bigg|_{q=0}\\ &- \frac{\big(4\beta p^2\big(\frac{N-3}{N}\big)\sinh\big[2\beta p^2\big(\frac{N-3}{N}\big)q\big] - 4\beta^2p^2\big(\frac{N-2}{N^2}\big)\big\{1-\tanh^2\big[\beta p^2\big(\frac{N-2}{N}\big)q\big]\big\}e^{-2\beta\frac{\langle s\rangle}{N}}\big)\big(2\cosh\big[2\big(\frac{N-3}{N}\big)\beta p^2q\big] - 2e^{-2\beta\langle s\rangle}\big)}{\big(2\cosh\big[2\beta p^2\frac{N-3}{N}q\big] + 2e^{-2\beta\frac{\langle s\rangle}{N}}\big)^2}\bigg|_{q=0}\\ &= \beta^2p^2\bigg(\frac{N-2}{N^2}\bigg).\end{aligned} \tag{C1}$$

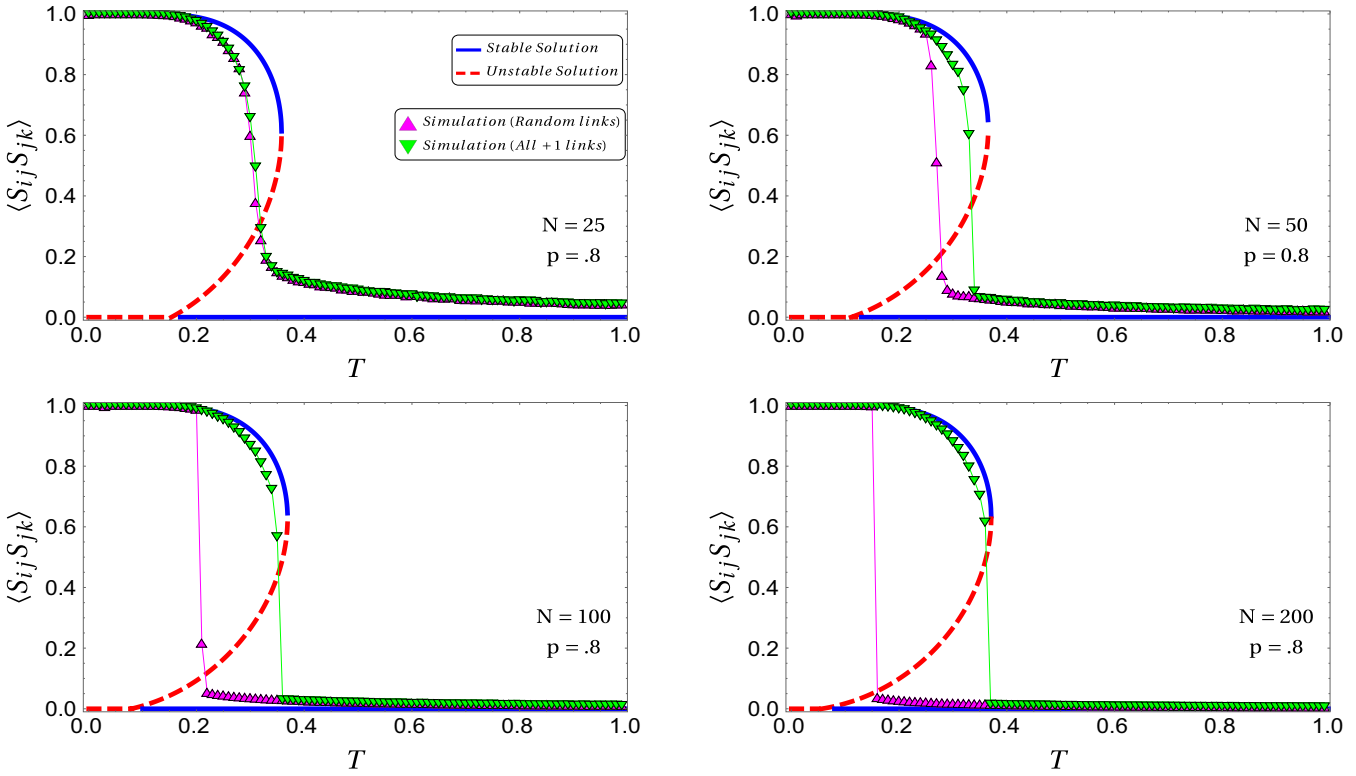

FIG. 7. Compatibility between Monte Carlo simulation (triangle-line curves) and mean-field solution (blue solid and red dashed curves) for the mean of two stars versus temperature. We have considered four ER random networks with $N = 25$, 50, 100, and 200 nodes with the connection probability $p = 0.8$.

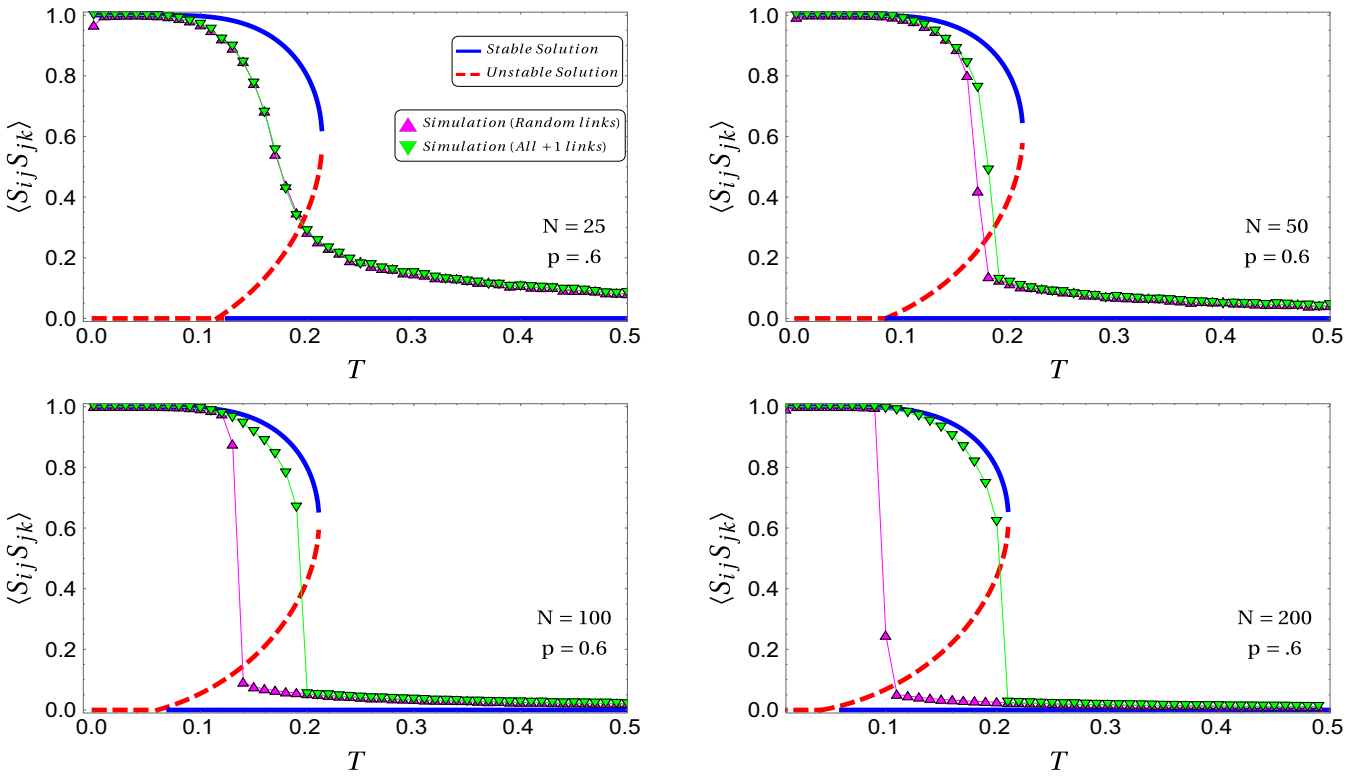

FIG. 8. Compatibility between Monte Carlo simulation (triangle-line curves) and mean-field solution (blue solid and red dashed curves) for the mean of two-stars versus temperature. We have considered four *ER* random networks with $N = 25$, 50, 100, and 200 nodes with connection probability $p = 0.6$.

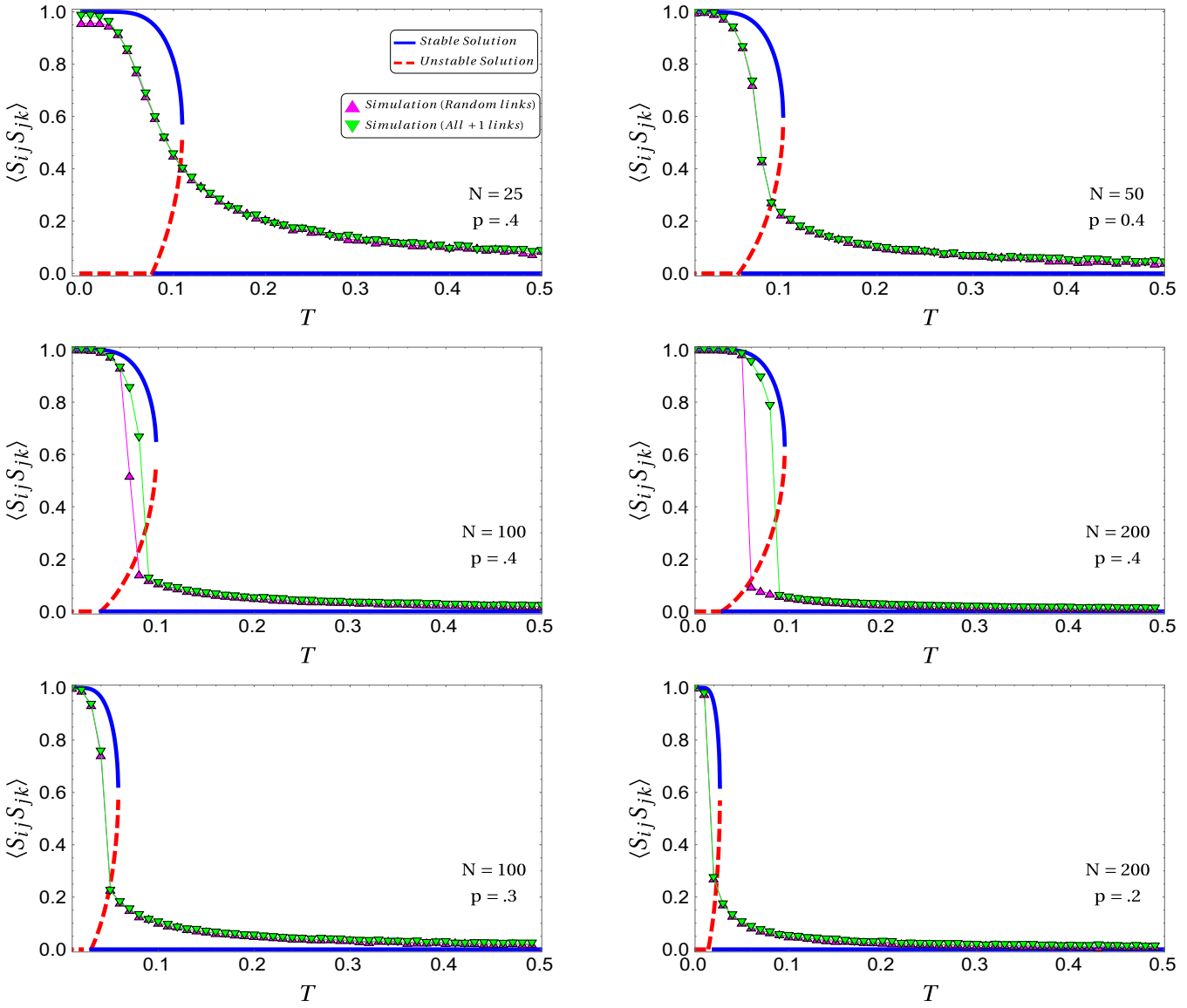

FIG. 9. Compatibility between Monte Carlo simulation (triangle-line curves) and mean-field solution (blue solid and red dashed curves) for the mean of two stars versus temperature. We have considered four ER random networks with $N = 25$, 50, 100, and 200 nodes with connection probabilities $p = 0.4$, 0.3, and 0.2.

Now if we apply $f'(q^* = 0) < 1$, we have

$$T_{\text{cold}} = p\sqrt{\frac{N-2}{N^2}}.$$

APPENDIX D: GRAPHICAL REPRESENTATION FOR SELF-CONSISTENT EQ. (16) FOR DIFFERENT CONNECTION PROBABILITY

In Fig. 4 we have illustrated the graphical representation of Eq. (16) for different connection probabilities. There is a single stable fixed point for $T < T_{\text{cold}}$ and $T > T_{\text{hot}}$, which represent the balanced and random phase, respectively. When $T_{\text{cold}} < T < T_{\text{hot}}$ we have two stable fixed points that represent the coexistence regions. Therefore, the number of intersections of Eq. (16) truly demonstrates the phase of our random network.

APPENDIX E: MEAN OF ENERGY DURING THE EVOLUTION OF AN ERDÖS-RÉNYI RANDOM NETWORK WITH DIFFERENT CONNECTION PROBABILITIES

Figure 5 illustrates the mean of energy during the evolution of an Erdös-Rényi (ER) random network of size $N = 50$ with connection probabilities $p = 1$, 0.8, 0.6, and 0.4 for a single trial. L represents every N^2 Monte Carlo step in Fig. 5. We have considered N^3 Monte Carlo steps for each realization of an ER random network to ensure that the network reaches its stationary state. The rationale for taking N^3 Monte Carlo steps is the number of triangles in an ER random network. As shown

in Fig. 5, the system reaches its stationary state after $10 * L$ steps.

APPENDIX F: COMPATIBILITY BETWEEN MEAN-FIELD SOLUTION AND MONTE CARLO SIMULATION

To show the correspondence between analytical and simulation results, we have prepared four figures for the mean of two stars versus temperature. As shown in Figs. 6–9 with increasing N, the agreement between analytical and Monte Carlo methods for predicting T_{hot} and T_{cold} increases; however, a slight mismatch for T_{cold} is observed even for $N = 200$. Since the basin of attraction of $q^* = o$, which corresponds to the random state, is narrow, this fixed point cannot be thoroughly captured in the simulations.

[1] M. Szell, R. Lambiotte, and S. Thurner, Proc. Natl. Acad. Sci. USA **107**, 13636 (2010).
[2] P. Singh, S. Sreenivasan, B. K. Szymanski, and G. Korniss, Phys. Rev. E **93**, 042306 (2016).
[3] G. Facchetti, G. Iacono, and C. Altafini, Proc. Natl. Acad. Sci. USA **108**, 20953 (2011).
[4] C. Altafini, PLoS One **7**, e38135 (2012).
[5] M. J. Krawczyk, M. Wołoszyn, P. Gronek, K. Kułakowski, and J. Mucha, Sci. Rep. **9**, 11202 (2019).
[6] T. M. Pham, I. Kondor, R. Hanel, and S. Thurner, Journal of the Royal Society Interface **17**, 20200752 (2020).
[7] R. Shojaei, P. Manshour, and A. Montakhab, Phys. Rev. E **100**, 022303 (2019).
[8] M. Saeedian, N. Azimi-Tafreshi, G. R. Jafari, and J. Kertesz, Phys. Rev. E **95**, 022314 (2017).
[9] J. Hart, J. Peace Res. **11**, 229 (1974).
[10] S. Galam, Phys. A (Amsterdam, Neth.) **230**, 174 (1996).
[11] A. Bramson, K. Hoefman, M. van den Heuvel, B. Vandermarliere, and K. Schoors, Measuring propagation with temporal webs, in *Temporal Network Epidemiology* (Springer, Singapore, 2017), pp. 57–104.
[12] E. Estrada, Discrete Appl. Math. **268**, 70 (2019).
[13] P. Doreian and A. Mrvar, J. Soc. Struct. **16**, 1 (2015).
[14] S. Aref and Z. Neal, Sci. Rep. **10**, 1506 (2020).
[15] H. Saiz, J. Gómez-Gardeñes, P. Nuche, A. Girón, Y. Pueyo, and C. L. Alados, Ecography **40**, 733 (2017).
[16] F. Heider, J. Psychol. **21**, 107 (1946).
[17] D. Cartwright and F. Harary, Psychol. Rev. **63**, 277 (1956).
[18] T. Antal, P. L. Krapivsky, and S. Redner, Phys. Rev. E **72**, 036121 (2005).
[19] K. Kułakowski, P. Gawroński, and P. Gronek, Int. J. Mod. Phys. C **16**, 707 (2005).
[20] S. A. Marvel, J. Kleinberg, R. D. Kleinberg, and S. H. Strogatz, Proc. Natl. Acad. Sci. USA **108**, 1771, (2010).
[21] F. Rabbani, A. H. Shirazi, and G. R. Jafari, Phys. Rev. E **99**, 062302 (2019).
[22] A. M. Belaza, K. Hoefman, J. Ryckebusch, A. Bramson, M. van den Heuvel, and K. Schoors, PLoS One **12**, e0183696 (2017).
[23] A. M. Belaza, J. Ryckebusch, A. Bramson, C. Casert, K. Hoefman, K. Schoors, M. van den Heuvel, and B. Vandermarliere, Phys. A (Amsterdam, Neth.) **518**, 270 (2019).
[24] V. M. Yakovenko and J. B. Rosser, Rev. Mod. Phys. **81**, 1703 (2009).
[25] W. A. Brock and S. N. Durlauf, Rev. Econ. Stud. **68**, 235 (2001).
[26] S. N. Durlauf and Y. M. Ioannides, Annu. Rev. Econ. **2**, 451 (2010).
[27] A. Hosseiny, M. Bahrami, A. Palestrini, and M. Gallegati, PLoS One **11**, e0160363 (2016).
[28] S. Galam and S. Moscovici, Eur. J. Soc. Psychol **21**, 49 (1991).
[29] M. Bahrami, N. Chinichian, A. Hosseiny, G. Jafari, and M. Ausloos, Phys. A (Amsterdam, Neth.) **540**, 123203 (2020).
[30] A. Kargaran, M. Ebrahimi, M. Riazi, A. Hosseiny, and G. R. Jafari, Phys. Rev. E **102**, 012310 (2020).
[31] R. Masoumi, F. Oloomi, A. Kargaran, A. Hosseiny, and G. R. Jafari, Phys. Rev. E **103**, 052301 (2021).
[32] F. Oloomi, A. Kargaran, A. Hosseiny, and G. R. Jafari, arXiv:2111.09092.
[33] M. Bagherikalhor, A. Kargaran, A. H. Shirazi, and G. R. Jafari, Phys. Rev. E **103**, 032305 (2021).
[34] F. Hassanibesheli, L. Hedayatifar, H. Safdari, M. Ausloos, and G. R. Jafari, Entropy **19**, 246 (2017).
[35] Y. Moreno, R. Pastor-Satorras, and A. Vespignani, Eur. Phys. J. B **26**, 521 (2002).
[36] R. Pastor-Satorras and A. Vespignani, Phys. Rev. Lett. **86**, 3200 (2001).
[37] C. Moore and M. E. J. Newman, Phys. Rev. E **61**, 5678 (2000).
[38] M. Woloszyn and K. Malarz, Phys. Rev. E **105**, 024301 (2022).
[39] P. Erdos and A. Reyni, Publ. Math. Inst. Hung. Acad. Sci **5**, 17 (1960).
[40] H. Nishimori, *Statistical Physics of Spin Glasses and Information Processing: An Introduction* (Clarendon Press, Oxford, 2001).